

Supplemental materials to

Source apportionment of particle number size distribution at the street canyon and urban background sites

5 Sami D. Harni^{1*}, Minna Aurela¹, Sanna Saarikoski¹, Jarkko Niemi², Harri Portin², Hanna Manninen²,
Ville Leinonen³, Pasi Aalto⁴, Phil Hopke⁵, Tuukka Petäjä⁴, Topi Rönkkö⁶, Hilkka Timonen¹

¹ Atmospheric Composition Research, Finnish Meteorological Institute, Helsinki, Finland

² Helsinki Region Environmental Services Authority (HSY), Helsinki, Finland

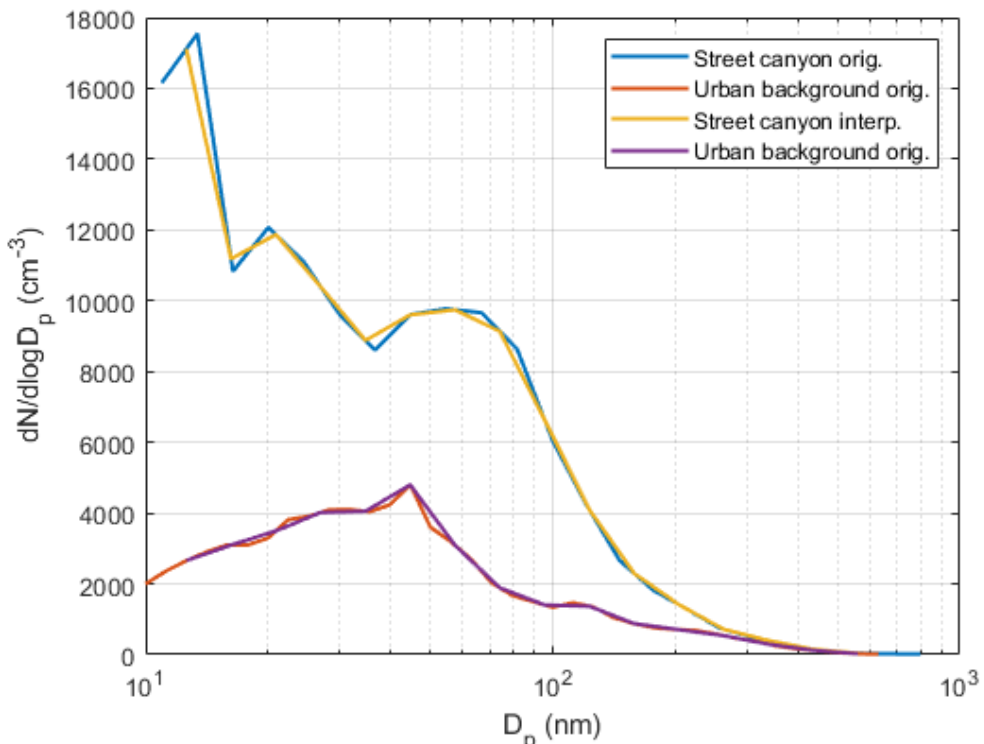
³ Faculty of Science, Forestry and Technology, Department of Technical Physics, University of Eastern Finland, Finland

10 ⁴ Institute for Atmospheric and Earth System Research (INAR) / Physics, Faculty of Science, University of Helsinki, Finland

⁵ Department of Public Health Sciences, University of Rochester School of Medicine and Dentistry, Rochester, NY 14642,
USA

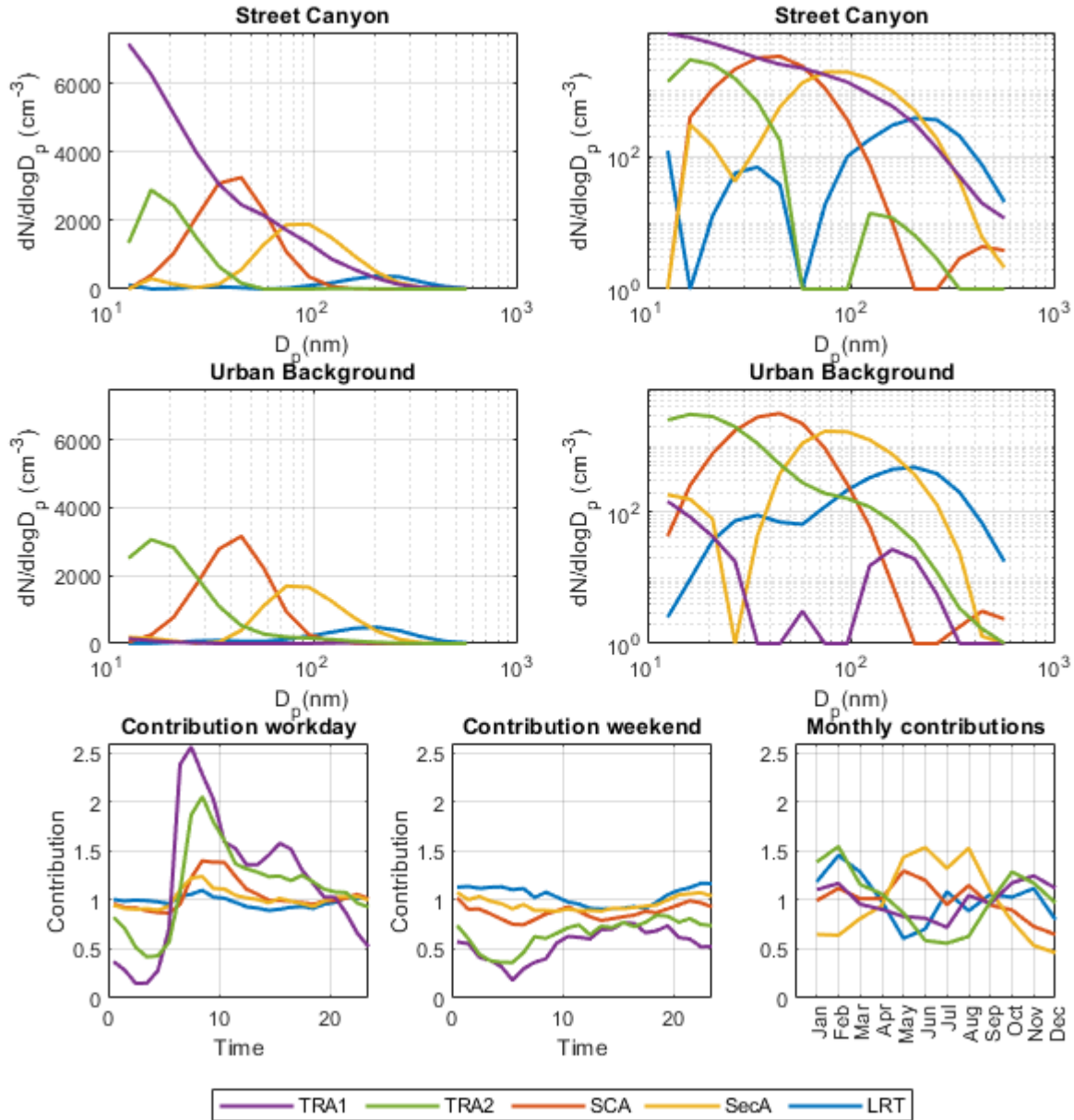
⁶ Aerosol Physics Laboratory, Tampere University, Tampere, Finland

Corresponding author: Sami D. Harni, sami.harni@fmi.fi

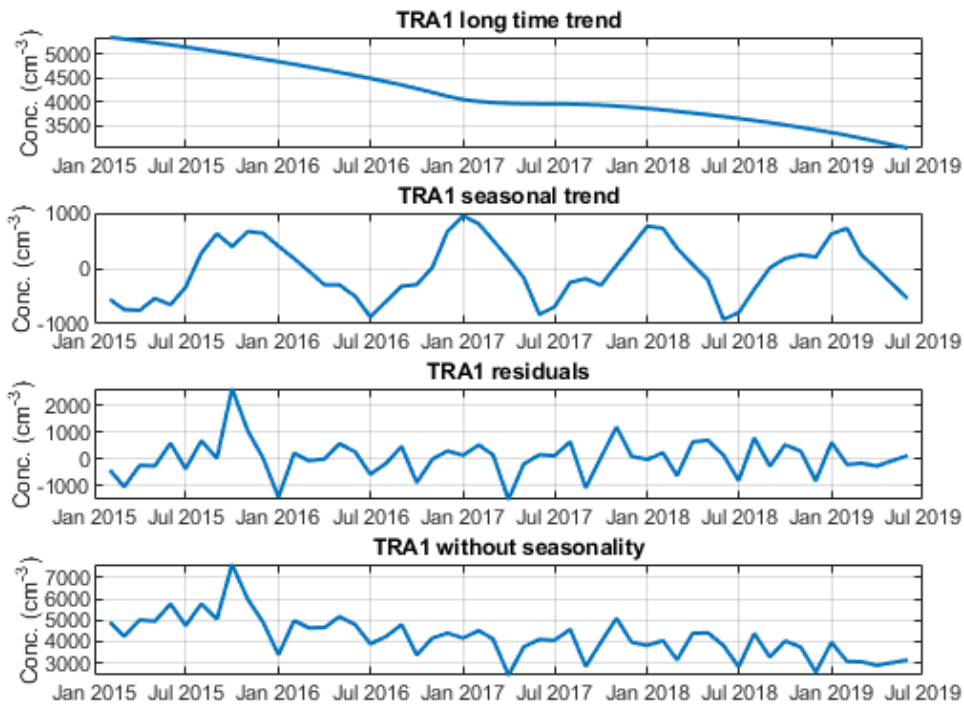


15

Figure S1: Example of 1 h average data the original data compared to the interpolated data for Street Canyon and Urban background sites.



20 Figure S2: Dispersion normalized Positive matrix factorization (PMF) factors presented in linear and logarithmic y-axes for Street Canyon (upper plot) and Urban background (middle plot) sites and their hourly relative contributions (lower plot) during workdays, weekends, and months. Note that the linear scale for the plots is different. The value presented in contribution figures is the factor with which to multiply the factor profile at any current time to get the total contribution. The average for the contribution factor is 1 over the whole measurement period for all the factors.



25 Figure S3: Decomposition of TRA1 factor time series into long-time trend, seasonal trend, and residuals using Seasonal-Trend Decomposition Procedure Based on Loess (Cleveland, et al., 1990). The lowest figure shows the TRA1 factor time series with the seasonality removed.

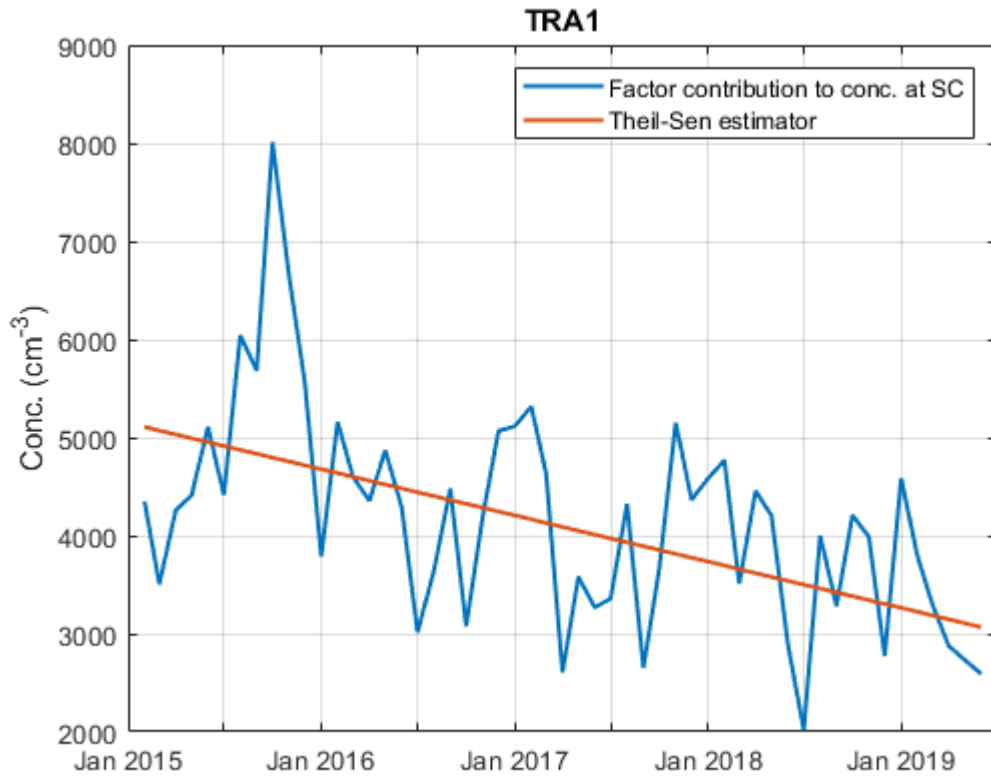
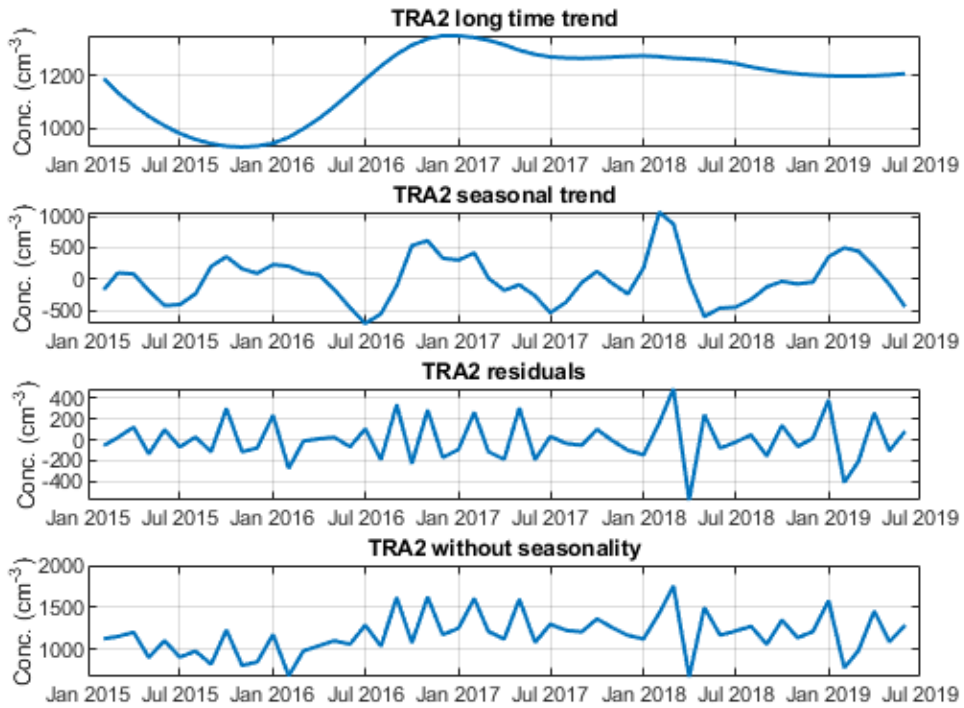
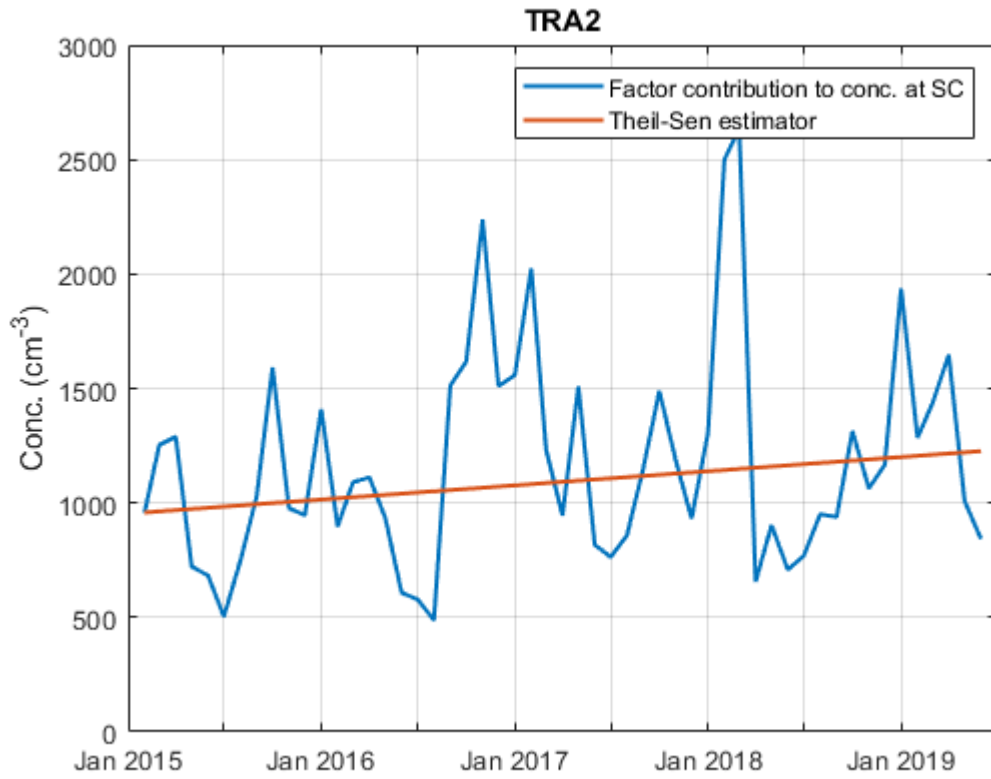


Figure S4: TRA1 factor time series and the fitted Theil-Sen estimator.



30

Figure S5: Decomposition of TRA2 factor time series into long-time trend, seasonal trend, and residuals using Seasonal-Trend Decomposition Procedure Based on Loess (Cleveland, et al., 1990). The lowest figure shows the TRA2 factor time series with the seasonality removed.



35 **Figure S6: TRA2 factor time series and the fitted Theil-Sen estimator.**

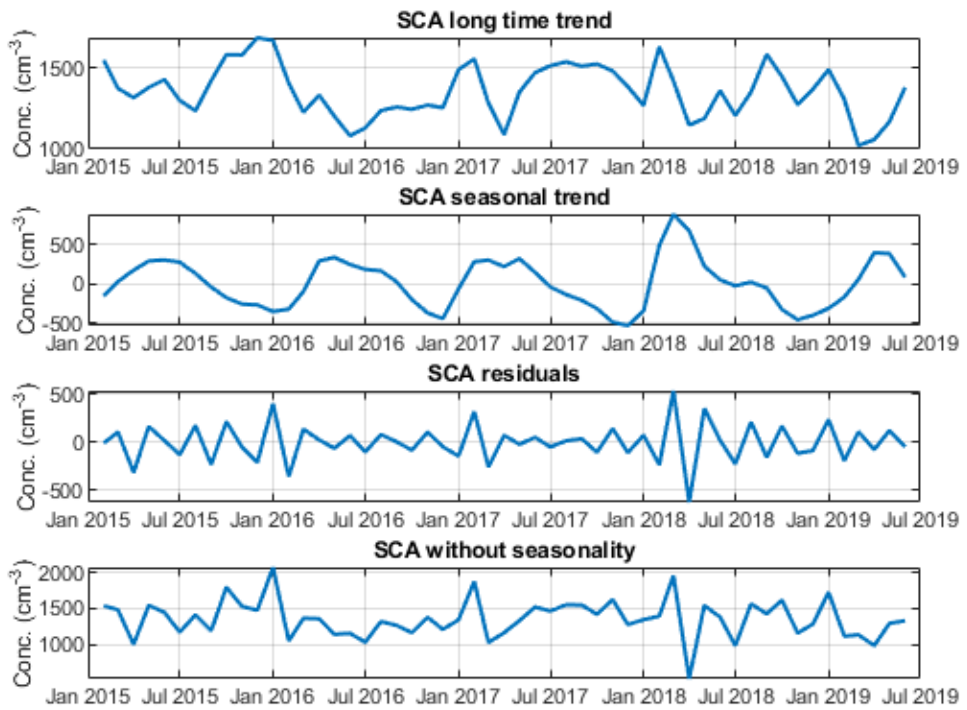


Figure S7: Decomposition of SCA factor time series into long-time trend, seasonal trend, and residuals using Seasonal-Trend Decomposition Procedure Based on Loess (Cleveland, et al., 1990). The lowest figure shows the SCA factor time series with the seasonality removed.

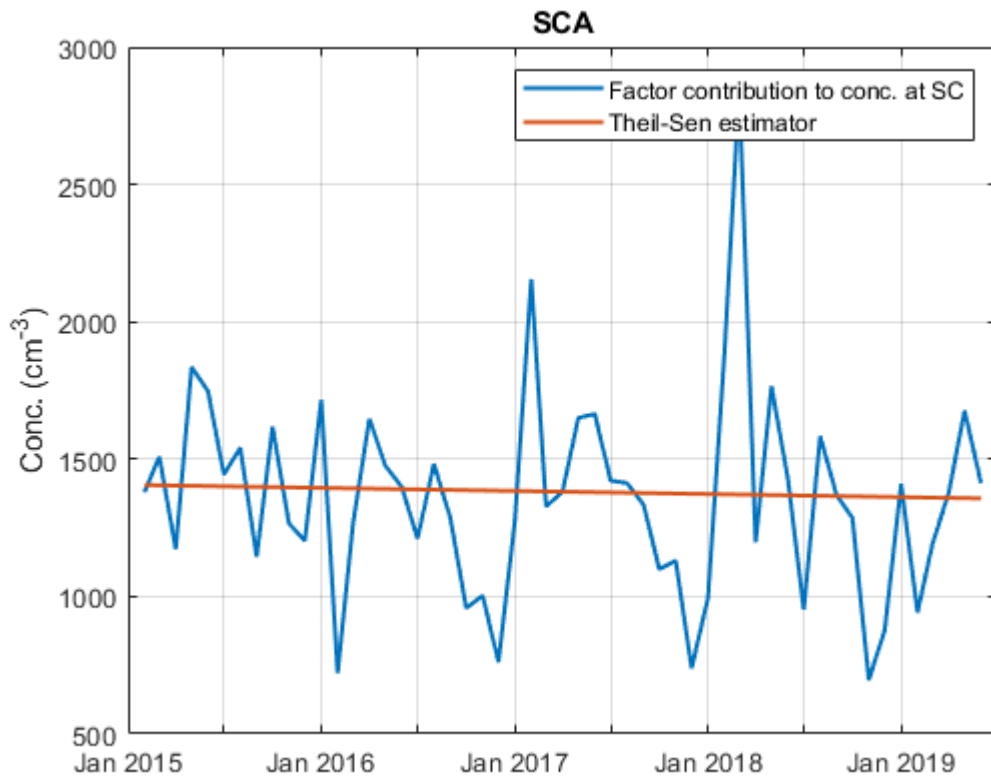
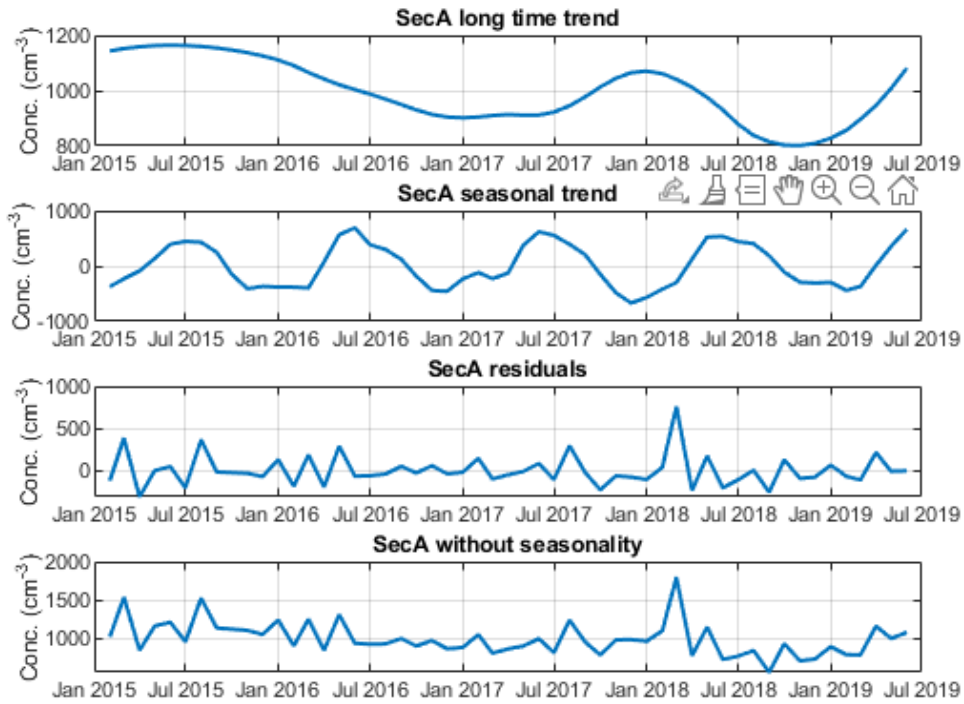


Figure S8: SCA factor time series and the fitted Theil-Sen estimator.



45 **Figure S9: Decomposition of SecA factor time series into long-time trend, seasonal trend, and residuals using Seasonal-Trend Decomposition Procedure Based on Loess (Cleveland, et al., 1990). The lowest figure shows the SecA factor time series with the seasonality removed.**

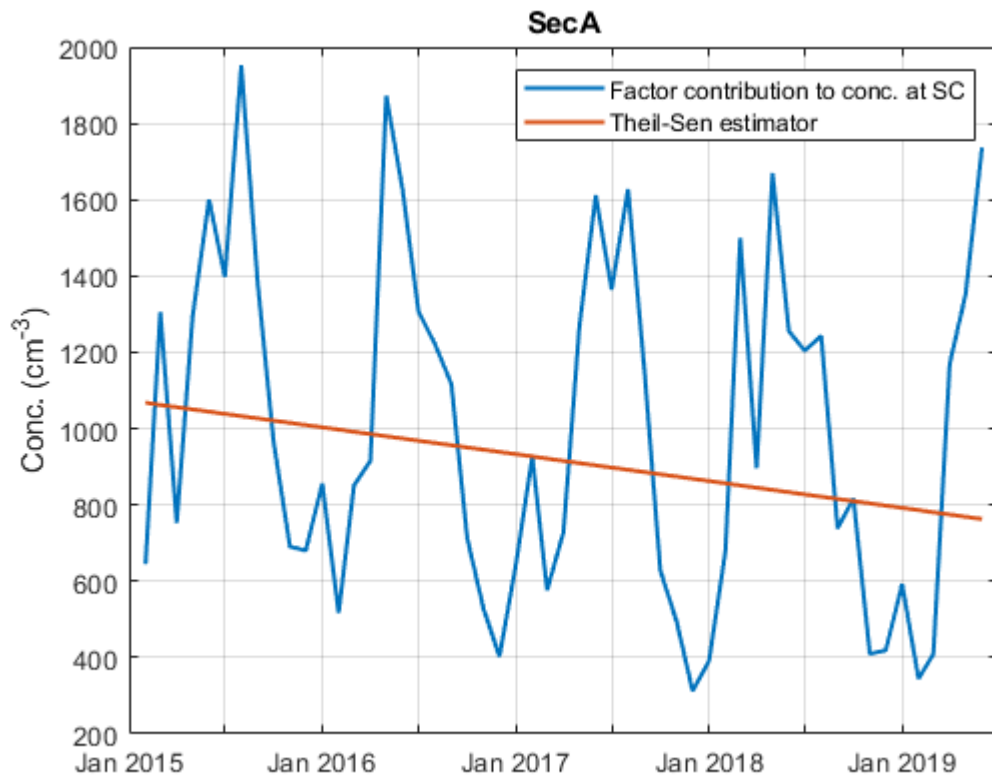
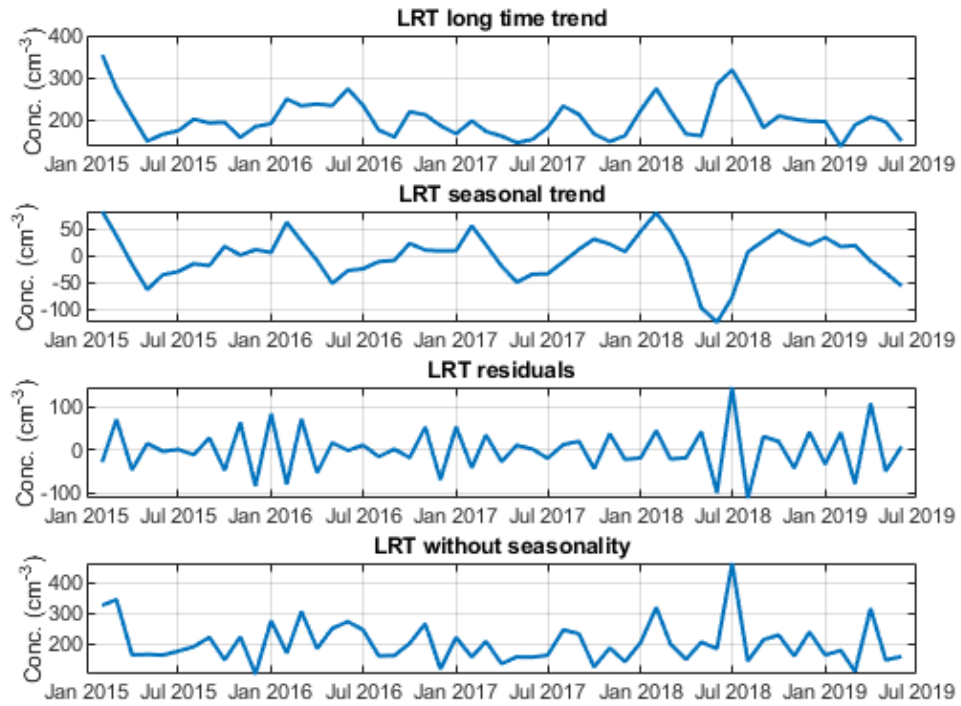
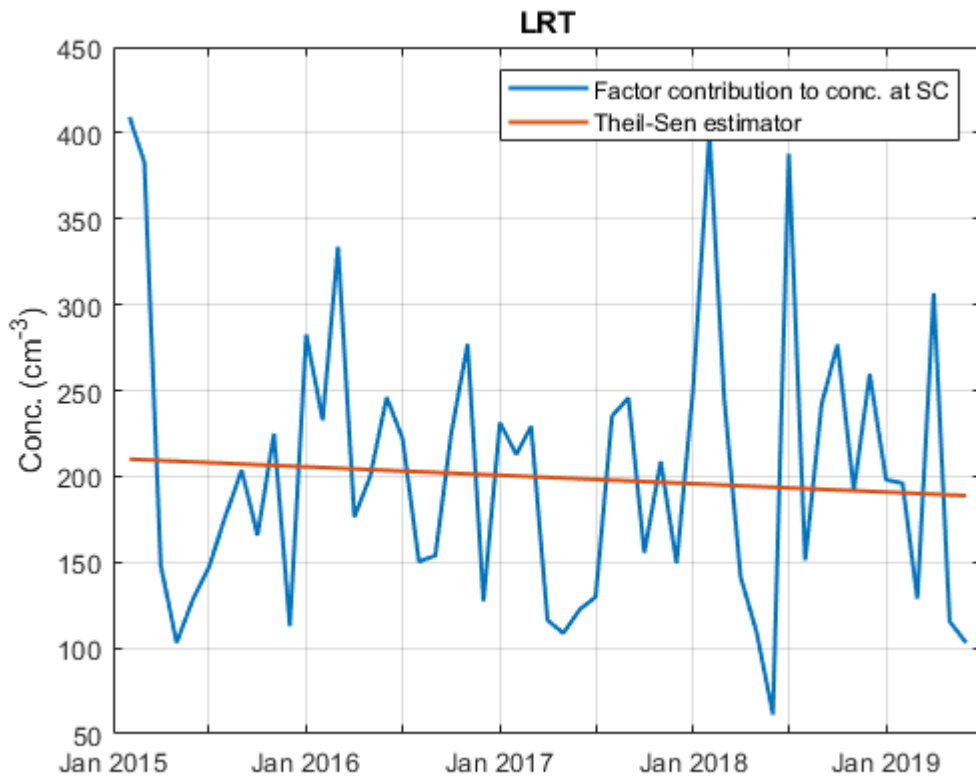


Figure S10: SecA factor time series and the fitted Theil-Sen estimator.



50 **Figure S11: Decomposition of LRT factor time series into long-time trend, seasonal trend, and residuals using Seasonal-Trend Decomposition Procedure Based on Loess (Cleveland, et al., 1990). The lowest figure shows the LRT factor time series with the seasonality removed.**



55

Figure S12: LRT factor time series and the fitted Theil-Sen estimator.

References

Cleveland, R. B., Cleveland, W. S., & Terpenning, I.: STL: A seasonal-trend decomposition procedure based on loess. *J. Off. Stat.*, 6(1), 3., 1990.

60